NANOS-3 and FBF proteins physically interact to control the sperm–oocyte switch in *Caenorhabditis elegans*

Brian Kraemer*†, Sarah Crittenden†‡, Maria Gallegos*§, Gary Moulder¶, Robert Barstead¶, Judith Kimble*‡¥ and Marvin Wickens*

Background: The *Caenorhabditis elegans* FBF protein and its *Drosophila* relative, Pumilio, define a large family of eukaryotic RNA-binding proteins. By binding regulatory elements in the 3′ untranslated regions (UTRs) of their cognate RNAs, FBF and Pumilio have key post-transcriptional roles in early developmental decisions. In *C. elegans*, FBF is required for repression of *fem-3* mRNA to achieve the hermaphrodite switch from spermatogenesis to oogenesis.

Results: We report here that FBF and NANOS-3 (NOS-3), one of three *C. elegans* Nanos homologs, interact with each other in both yeast two-hybrid and *in vitro* assays. We have delineated the portions of each protein required for this interaction. Worms lacking *nanos* function were derived either by RNA-mediated interference (*nos-1* and *nos-2*) or by use of a deletion mutant (*nos-3*). The roles of the three *nos* genes overlap during germ-line development. In certain *nos*-deficient animals, the hermaphrodite sperm–oocyte switch was defective, leading to the production of excess sperm and no oocytes. In other *nos*-deficient animals, the entire germ line died during larval development. This germ-line death did not require CED-3, a protease required for apoptosis.

Conclusions: The data suggest that NOS-3 participates in the sperm–oocyte switch through its physical interaction with FBF, forming a regulatory complex that controls *fem-3* mRNA. NOS-1 and NOS-2 also function in the switch, but do not interact directly with FBF. The three *C. elegans nanos* genes, like *Drosophila nanos*, are also critical for germ-line survival. We propose that this may have been the primitive function of *nanos* genes.

Addresses: *Department of Biochemistry, ‡Howard Hughes Medical Institute and ¥Laboratory of Molecular Biology and Department of Medical Genetics, University of Wisconsin-Madison, Madison, Wisconsin 53706, USA. ¶Program in Molecular Biology, Oklahoma Medical Research Foundation, Oklahoma City, Oklahoma 73104, USA.

§Present address: Department of Anatomy, University of California-San Francisco, San Francisco, California 94143, USA.

†B.K. and S.C. contributed equally to this work.

Correspondence: Marvin Wickens
E-mail: wickens@biochem.wisc.edu

Received: 8 July 1999
Revised: 5 August 1999
Accepted: 9 August 1999

Published: 9 September 1999

Current Biology 1999, 9:1009–1018
http://biomednet.com/elecref/0960982200901009

0960-9822/99/$ – see front matter

Background

In the germ line and early embryo, post-transcriptional controls are responsible for key developmental decisions, including patterning and establishment of cell fates [1–4]. These controls are often mediated by specific regulatory elements in the 3′ untranslated region (UTR) that govern an mRNA's translational activity, stability and cellular location.

The *Caenorhabditis elegans* FBF protein and *Drosophila* Pumilio define a family of related RNA-binding proteins called Puf proteins that are found throughout the eukaryotic kingdom [5]. Their functions are best understood in *C. elegans* and *Drosophila*. FBF binds specifically to a regulatory element of the *fem-3* mRNA that controls the sperm–oocyte switch in *C. elegans* hermaphrodites [5–7]. Normally, hermaphrodites make sperm first and then switch to oogenesis. In gain-of-function mutants that disrupt a regulatory element in the *fem-3* 3′UTR, the switch does not occur, and sperm are made continuously. FBF is a repressor that binds specifically to that regulatory element in the *fem-3* 3′UTR. Pumilio was first identified as a gene that regulates patterning in the early *Drosophila* embryo [8], but more recently has been found to control germ-line stem-cell divisions [9,10]. Its role in patterning requires its specific interaction with regulatory elements in the 3′UTR of *hunchback* mRNA, leading to translational repression of that mRNA [11–14]. Although elegant genetic analyses establish that repression by Pumilio requires *nanos* gene activity, the molecular nature of this collaboration remains unknown.

Here, we demonstrate that FBF physically interacts with a *C. elegans* Nanos homolog, and characterize the biological roles of this and two other *nanos* orthologs present in the *C. elegans* genome. We originally identified NANOS-3 (NOS-3) using a yeast two-hybrid screen with FBF as bait. This physical interaction was confirmed using *in vitro* assays. Neither NOS-1 nor NOS-2 interacted detectably with FBF by either assay. Importantly, all three *nanos* (*nos*) genes play a role in controlling the sperm–oocyte switch. We suggest that NOS proteins act in a redundant fashion to control *fem-3* post-transcriptionally, and that FBF and NOS-3 do so in a regulatory complex. Moreover, we found that the NOS proteins promote germ-line survival. Because *Drosophila* Nanos similarly

Figure 1

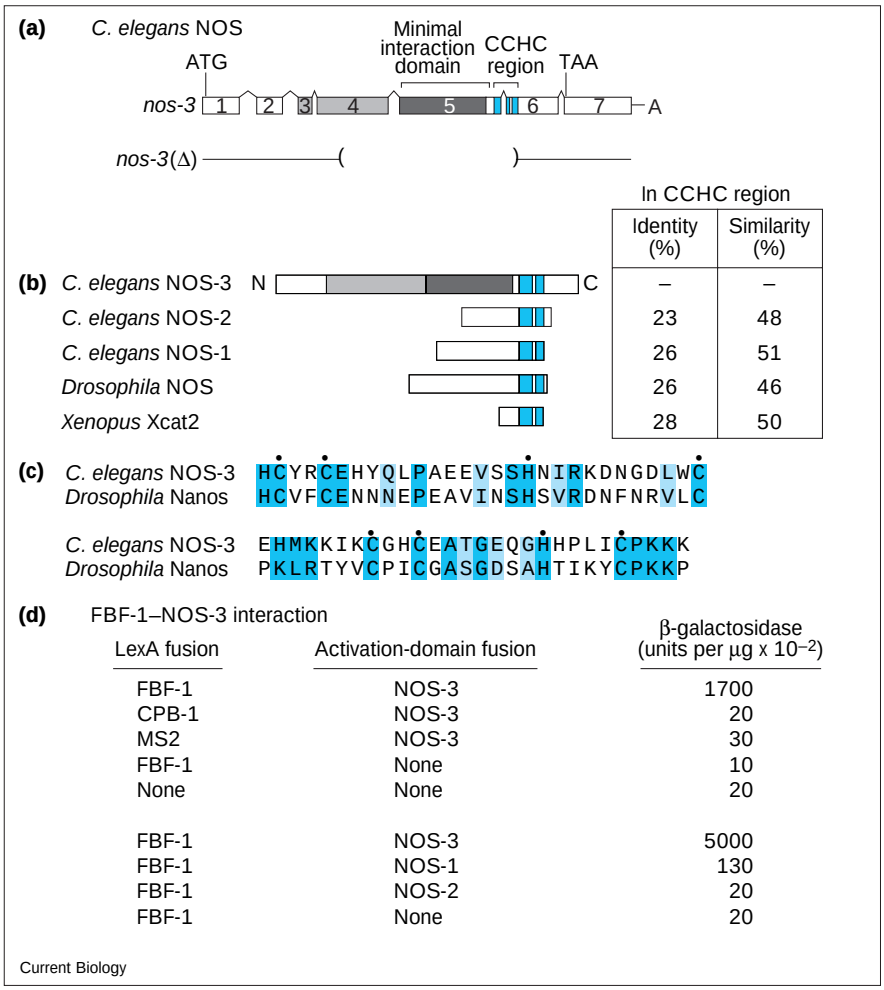

NOS-3 interacts with FBF. (a–c) The *nos-3* mRNA and protein. (a) Schematic illustration of the *nos-3* pre-mRNA and the *nos-3*(Δ) mutation. Boxes, exons; lines, introns; blue, putative CCHC zinc fingers (each is indicated as a block); dark grey, minimal region required for interaction with FBF-1 (amino-acid residues 429–681; see Figure 2); light grey, region that enhances interaction with FBF-1 (amino acids 192–428; see Figure 2); ATG and TAA, initiation and termination codons, respectively. NOS-3 contains polyglutamate stretches in its amino-terminal half, as does *Drosophila* Nanos [42]. Shown below (*nos-3*(Δ)) is the chromosomal deletion *nos-3(q650)*, which removes the minimal FBF-interaction domain, first zinc finger and half of the second zinc finger, and shifts the downstream sequence out of frame. The predicted deletion protein contains amino acids 1–286 plus 31 extra amino acids from the frameshift. (b) Schematic illustration of the proteins encoded by the three *C. elegans nos* genes, *Drosophila nanos* and *Xenopus Xcat2*. N, amino terminus; C, carboxyl terminus. The respective amino-acid identities and similarities in the CCHC region are indicated on the right. NOS-1 and NOS-2 contain 312 and 260 amino acids, respectively. (c) Alignment of amino-acid sequences in the CCHC regions of *C. elegans* NOS-3 and *Drosophila* Nanos. Dark and light shading, identical and similar amino acids, respectively; black dots, CCHC residues. (d) FBF-1–NOS-3 interaction in the yeast two-hybrid system. FBF-1 (amino acids 121–614), NOS-3 (amino acids 42–871), NOS-1 (amino acids 1–311), NOS-2 (amino acids 1–259), CPB-1, a *C. elegans* ortholog of cytoplasmic polyadenylation element binding protein (amino acids 1–560; C. Luitjens, J.K and M.W., unpublished data) and MS2 coat protein (amino acids 1–131; [43,44]) were tested in the yeast two-hybrid system, using fusions to the LexA DNA-binding domain and Gal4 transcriptional-activation domain. The third column shows β-galactosidase enzyme activity per μg of yeast lysate protein [34].

affects germ-line viability [10,15], we suggest that this might have been the primitive function of the *nos* genes.

Results

NOS-3 and FBF proteins interact physically

We used a fusion protein between FBF-1 and the DNA-binding domain of Lex A (Lex A–FBF-1) as bait in a yeast two-hybrid screen to identify nematode proteins that interact with FBF-1. Of the 20,000,000 independent cDNA transformants screened, 19 were found that activated both the *HIS3* and *lacZ* reporter genes in the presence of LexA–FBF-1, but not in the presence of a fusion protein between LexA and the MS2 coat protein. Three independently isolated cDNAs were found to be derived from a single gene related in sequence to *Drosophila* Nanos. We refer to this nematode gene as *nos-3*.

The complete sequence of the longest *nos-3* cDNA was determined, and its splicing pattern deduced by comparison with the genomic sequence [16] (Figure 1a). The 5′ and 3′ termini were determined by rapid amplification of cDNA ends (RACE) and oligo(dT)-primed RT–PCR, respectively. The *nos-3* mRNA contains seven exons and encodes a protein of 871 amino acids. Sequence similarity between *C. elegans* NOS-3 protein and *Drosophila* Nanos was confined to the carboxy-terminal region, which contained two distinctive CCHC zinc fingers that are diagnostic of proteins in the NOS family (Figure 1a–c) [17]. These CCHC residues are required for *Drosophila* Nanos to regulate *hunchback* mRNA, and to bind non-specifically to RNA [18,19].

FBF-1 and NOS-3 interacted specifically in the yeast two-hybrid system: no interaction was detected when

Figure 2

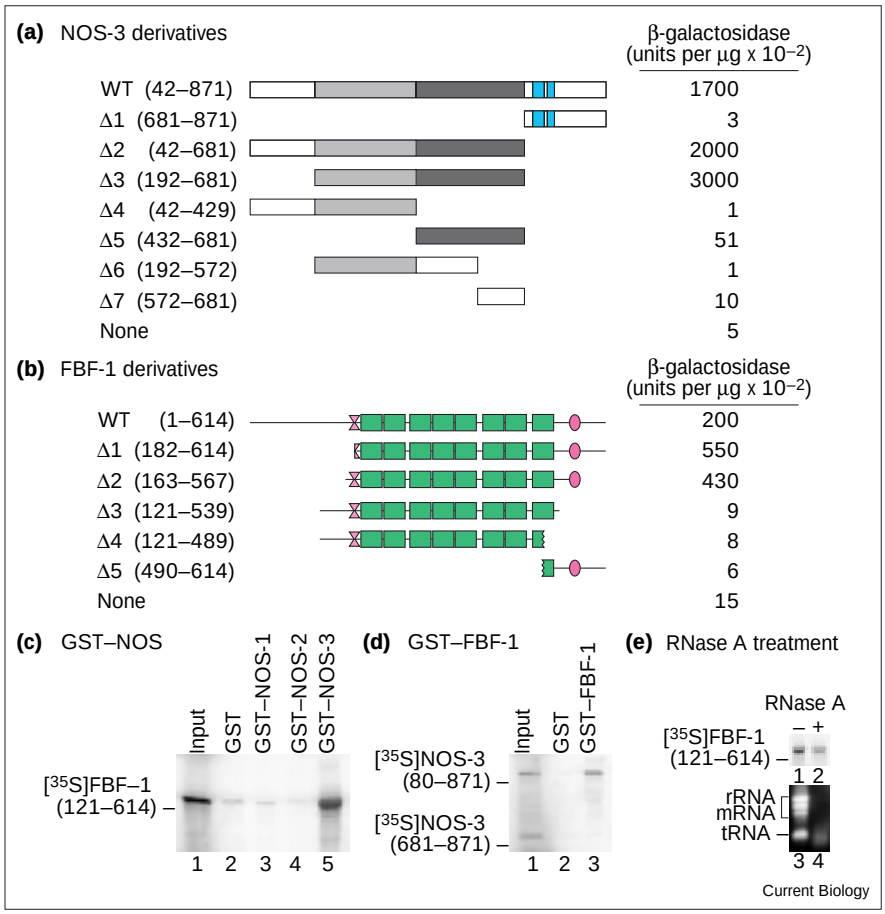

Regions required for the FBF-1–NOS-3 interaction. (a) NOS-3 domains required for the interaction with FBF-1 in the yeast two-hybrid system. The Gal4 activation-domain plasmid carrying wild-type (WT) NOS-3 or the indicated truncated derivatives (the amino-acid residues expressed are indicated in parentheses) was introduced into yeast expressing LexA–FBF-1 (121–614), a fusion protein between the DNA-binding domain of LexA and amino-acid residues 121–614 of FBF-1. None indicates a strain containing the activation-domain vector without an insert. Dark grey, minimal region required for interaction with FBF-1; light grey, region that enhances interaction with FBF-1; blue blocks, putative CCHC zinc fingers. (b) FBF-1 region required for interaction with NOS-3 in the yeast two-hybrid system. Full-length FBF-1 or the indicated truncated derivatives carried in the activation-domain plasmid were introduced into yeast containing LexA–NOS-3 (42–681). Green, the eight consecutive Puf repeats of FBF; pink anvil, Csp1; pink oval; Csp2. The eight Puf repeats, Csp1 and Csp2 regions are all required for binding to RNA [5]. (c) Interaction between GST–NOS fusion proteins and FBF-1. Fusion proteins consisting of GST fused to NOS-1 (amino acids 1–311), NOS-2 (amino acids 1–259) or NOS-3 (amino acids 432–681) were linked to beads and incubated with ^{35}S-labeled FBF-1 (amino acids 121–614) prepared by translation *in vitro*. Bound proteins were eluted and analyzed by electrophoresis. Protein immobilized on the beads is indicated above each lane. (d) Interaction between GST–FBF-1 and NOS-3 requires the NOS-3 interaction domain. GST–FBF-1 (121–614) was attached to beads, and incubated with a mixture of ^{35}S-labeled NOS-3 that was nearly full length (amino acids 80–871) or was missing the interaction domain (that is, contained amino acids 681–871), prepared by translation *in vitro*. Bound proteins were eluted and analyzed by electrophoresis. Protein immobilized on the beads is indicated above each lane. In (c,d) input (lane 1) indicates material before incubation with the GST protein (equivalent to 10% of the material analyzed in experimental lanes). (e) Interaction between NOS and FBF-1 persists after removal of RNA. Radiolabeled [^{35}S]FBF-1 (amino acids 121–614) was prepared by translation *in vitro*. The lysate containing FBF-1 was treated with RNase A, or incubated without the nuclease, before incubation with beads carrying GST–NOS-3 (amino acids 432–681). After RNase A treatment, an aliquot of the lysate was removed and deproteinized to detect endogenous RNAs using electrophoresis and staining with ethidine bromide. The lysate was incubated with GST–NOS-3 beads, and bound protein eluted and analyzed by electrophoresis. Lane 1, protein retained, no RNase A treatment; lane 2, protein retained, with RNase A treatment; lane 3, RNA in lysate, no RNase A treatment; lane 4, RNA in lysate, with RNase A treatment.

either partner was replaced by any of several different polypeptides (Figure 1d; data not shown). In addition, FBF-1 did not interact detectably with two other *C. elegans* NOS homologs, NOS-1 and NOS-2 (Figure 1d). NOS-3 interacted with FBF-2, a protein that is 91% identical to FBF-1 and that also binds to and regulates *fem-3* mRNA (data not shown; [5]).

The regions of NOS-3 and FBF-1 required for their interaction were identified by analyzing deletion derivatives of each protein in the yeast two-hybrid assay (Figure 2a). For NOS-3, a 249 amino-acid segment (residues 432–681, dark grey shading) that lies amino-terminal to the zinc-finger region was sufficient for binding FBF-1 (Figure 2a; Δ5). Inclusion of an additional 239 amino acids of NOS-3 further upstream (amino acids 192–431, light grey shading) enhanced the interaction to the level observed with the complete protein (Figure 2a; Δ3, light grey shading). The enhancing region did not interact significantly with FBF-1 (Figure 2a, Δ4 and Δ6). The interaction between the minimal FBF-binding domain of NOS-3 (Δ5, amino acids 432–681) and FBF-1 was specific: it was detected with either NOS-3 or FBF as the LexA fusion, and was not detected with either control or mutant NOS-3

proteins as partners (data not shown). For FBF-1, the region required for binding to NOS-3 was determined through comparable yeast two-hybrid studies, using LexA–NOS-3 and a collection of FBF-1 derivatives (Figure 2b). FBF-1 consists of eight repeats of approximately 40 amino acids; short conserved sequences, Csp1 and Csp2, are found amino-terminal to the first repeat and carboxy-terminal to the last repeat, respectively. These features are diagnostic of Puf proteins generally [5]. The eight conserved Puf repeats and flanking Csp regions of FBF-1 were sufficient for interaction with NOS-3 (Figure 2b, Δ2), as they are for RNA binding [5]. Removal of Csp2, on the carboxy-terminal side of the Puf repeats, abolished binding (Figure 2b, Δ3 and Δ4). Partial removal of Csp1, which greatly reduces FBF-1 binding to the *fem-3* RNA [5], had little or no effect on the interaction with NOS-3 (Figure 2b, Δ1).

To analyze the interaction between FBF-1 and NOS-3 *in vitro*, we performed affinity chromatography experiments using fusions of glutathione-S-transferase (GST) to NOS-3 or FBF-1 (Figure 2c,d). To this end, ^{35}S-labeled FBF-1 was produced by translation *in vitro*, and incubated with beads carrying GST fusions to NOS-1, NOS-2 or NOS-3. Radiolabeled FBF-1 bound to GST–NOS-3, but not to the other GST fusion proteins or to GST alone (Figure 2c, compare lane 5 with lanes 2–4). We also reversed the NOS and FBF-1 protein components (Figure 2d). Immobilized GST–FBF-1 was incubated with either a mixture of nearly full-length, ^{35}S-labeled NOS-3 (amino acids 80–871) or an amino-terminally deleted form of the protein (amino acids 681–871) lacking the portion of NOS-3 required to interact with FBF-1 in the two-hybrid system. The nearly full-length NOS-3 bound to GST–FBF, whereas the deleted version did not (Figure 2d).

The *in vitro* translation system used to produce ^{35}S-labeled protein contains RNAs, including rRNA and tRNA, as well as the mRNA added exogenously. In principle, although no RNAs containing *fem-3* sequences are present in the lysate, FBF-1 and NOS-3 might co-occupy an RNA through independent, non-specific RNA–protein interactions. To test this possibility, we treated a lysate containing ^{35}S-labeled FBF-1 with high levels of ribonuclease A (RNase A) before incubation with GST–NOS-3 (Figure 2e). RNase A treatment had little effect on the binding of GST–NOS-3 to FBF-1 (Figure 2e, lanes 1,2), yet resulted in the virtually complete degradation of rRNA in the lysate (Figure 2e, lanes 3,4). Furthermore, NOS-3 bound RNA non-specifically in the three-hybrid system, binding similarly to an irrelevant stem–loop structure (an iron response element) and the *fem-3* 3′UTR (data not shown). Further more, if the CCHC zinc-finger region is responsible for its non-specific RNA binding of *C. elegans* NOS, as is the case for *Drosophila* Nanos [18], the regions of NOS-3 that bind RNA are separable from those binding FBF-1.

We conclude that NOS-3 and FBF-1 proteins interact with one another, and that the interaction requires the central portion of NOS-3 and the Puf repeat region of FBF-1. In contrast, neither NOS-1 nor NOS-2 interacts detectably with FBF-1, consistent with the fact that they lack the interaction domain present in NOS-3.

The *nos-3* mRNA and protein are present in the germ line and present throughout development

FBF is required in *C. elegans* hermaphrodites for the sperm–oocyte switch: in its absence, sperm are made continuously and the switch to oogenesis does not occur [5]. We found that *nos-3* is expressed at the right time and place to participate with FBF in the sperm–oocyte switch (Figure 3). A 3.3 kb *nos-3* mRNA, which corresponds well to its predicted length (3,207 nucleotides), was present in wild-type animals, but barely detectable in animals lacking a germ line (Figure 3a, lanes 1,2). Therefore, *nos-3* mRNA is likely to reside primarily in the germ line, and to be expressed only at a low level in somatic tissue. Furthermore, *nos-3* mRNA was present throughout development, increasing in abundance at the L4 larval stage, just before oocytes first appear (Figure 3a, lanes 3–9).

Using affinity-purified antibodies, we detected NOS-3 protein throughout the germ-line tissue during larval development (Figures 3b,c; data not shown). Staining with anti-NOS-3 antibodies was specific, in that it was dramatically reduced in *nos-3* deletion mutants (compare Figure 3b with Figure 3e). At all stages of germ-line development, NOS-3 was predominantly cytoplasmic: this was evidenced by the dark, non-staining 'holes' corresponding to nuclei in the germ line at the larval L3 stage (Figure 3b). The distribution of NOS-3 overlapped with regions of the cytoplasm containing P granules, detected using anti-PGL-1 antibodies (Figure 3c,d; [20]); however, within the cytoplasm, NOS-3 staining was uniform and diffuse throughout. At the late L4 stage, NOS-3 was detected in germ cells in mitosis and meiotic pachytene, but decreased in the spermatogenic region (Figure 3h). In these experiments, mitotic cells were detected using antibodies against a phosphorylated form of histone H3 (Figure 3i; green) and sperm were marked with an anti-sperm antibody (Figure 3i; blue).

In addition to staining in the larval gonad, NOS-3 expression was also observed in embryos. Specifically, NOS-3 was found in P1–P4, early embryonic blastomeres that ultimately generate the germ line (Figure 3j–l, data not shown), and later in germ-line progenitor cells, Z2 and Z3 (data not shown). Although the distribution of NOS-3 in P cells was punctate, it did not precisely coincide with P granules (Figure 3j–l).

NOS functions in the hermaphrodite sperm–oocyte switch

If NOS-3 acts with FBF to repress *fem-3* to cause the hermaphrodite switch from spermatogenesis to oogenesis,

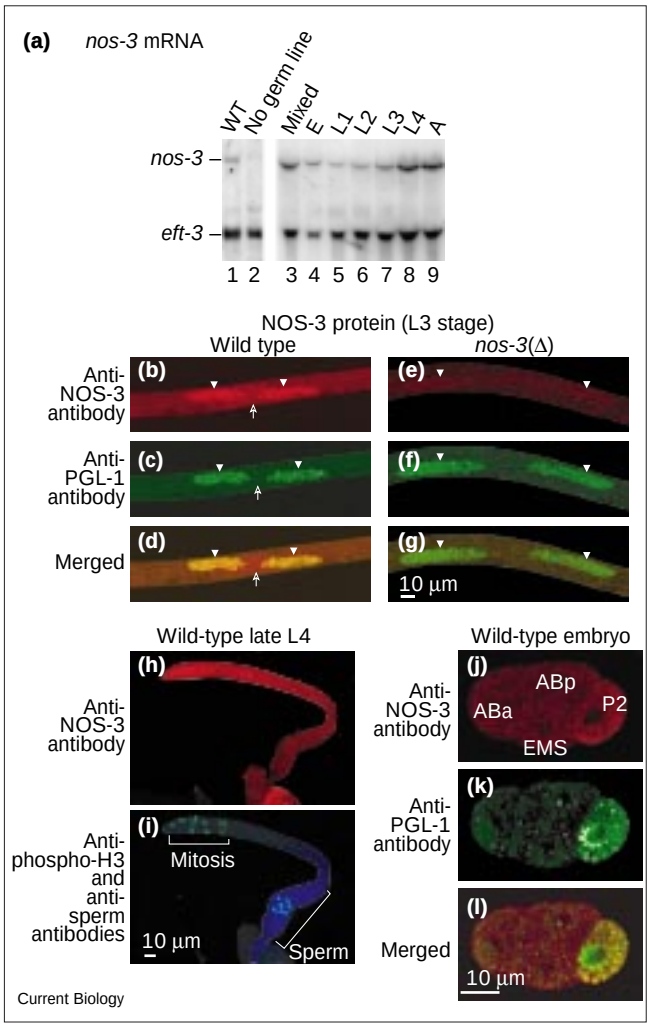

Figure 3

(a) Expression of *nos-3* mRNA. Polyadenylated *C. elegans* mRNA was separated through a 1% agarose glyoxal gel, transferred to a filter and probed with a *nos-3* cDNA. Lane 1, wild-type adults, which possess approximately 2,000 germ cells [45]; lane 2, *glp-1(q224)* mutant adults, which possess no more than eight germ cells [46]; lane 3, mixture of developmental stages (from first larval stage through adults with embryos); lanes 4–9, embryos (E), the four larval stages (L1–L4) and adults (A), respectively. In lane 2, note that very little *nos-3* mRNA is detectable; the small amount remaining may represent somatic expression. To verify equal loading of lanes, the blot was probed for expression of elongation factor-1α (*eft-3*). (b–g) NOS-3 protein expression in the gonads of L3 hermaphrodites. (b–d) Wild type and (e–g) *nos-3*(Δ) L3 larvae stained with (b,e) anti-NOS-3 and (c,f) anti-PGL-1 antibodies; (d,g) are the merged images of (b,c) and (e,f), respectively. At this stage, the germ line is proliferating; the *nos-3* mutant is slightly older than the wild type and thus has a slightly larger germ line. (b) NOS-3 protein was uniformly distributed throughout the cytoplasm in the anterior and posterior germ-line tubes of wild-type animals (arrowheads), and there was faint staining in the somatic gonadal tissue (arrow). (e) The protein was absent in *nos-3* mutants even though germ-line cells were present, as evidenced by (f) staining with anti-PGL-1 antibody, which is specific for P granules in the germ line [20]. (h,i) NOS-3 protein expression in the L4 hermaphrodite germ line. The germ-line tube of a wild-type late L4 hermaphrodite was extruded for staining. At this stage, spermatogenesis has begun. (h) NOS-3 protein was found in the germ-line cytoplasm and was most prominent in germ cells in mitosis and meiotic pachytene. (i) Mitotic nuclei were stained with an antibody against a phosphorylated form of histone H3 (anti-phospho-H3 antibody, green), and spermatogenic cells with an anti-sperm antibody called SP56 (blue). Sperm with highly condensed nuclei also stain with anti-phospho-histone antibody. (j–l) NOS-3 protein expression in the early embryo. A wild-type four-cell embryo is shown stained with antibodies against (j) NOS-3 and (k) PGL-1; (l) is the merged image with overlapping signals in yellow. (j) Each of the four blastomeres is indicated. NOS-3 was localized to the cytoplasm of P blastomeres, which generate the germ line. (k) PGL-1 is localized to P granules in the early embryo [20].

then animals lacking *nos-3* should produce sperm continuously and not switch to oogenesis. To test this prediction, we isolated a deletion of the *nos-3* gene (see Materials and methods). The *nos-3*(Δ) mutation (Figure 1a) removes 1381 nucleotides from the *nos-3* coding region; the predicted NOS-3(Δ) protein lacks the FBF-interacting region, all of the first zinc finger and half of the second, and truncates the protein 526 amino acids before the normal carboxyl terminus. The mRNA produced by *nos-3*(Δ) mutants was approximately 1.8 kb, in keeping with its predicted length of 1,826 nucleotides (data not shown). As with progeny of *nos-3* mutants generated by RNA-mediated interference (RNAi), *nos-3*(Δ) homozygotes were predominantly wild type, even when derived from a *nos-3*(Δ) homozygous mother. Continuous spermatogenesis without oogenesis was observed only rarely among *nos-3* homozygotes (<1%, $n > 2000$; Table 1, column 2); furthermore, among fertile *nos-3* mutants, the switch to oogenesis occurred at the correct time and the normal number of sperm were produced (as deduced from the average brood size of 278 per hermaphrodite; $n = 7$). No other defects were observed in either somatic or germ-line tissues, and no abnormalities were found in *nos-3*(Δ)/+ heterozygotes (data not shown). We conclude that *nos-3* can indeed influence the sperm–oocyte switch, but that it is not normally essential.

One possible explanation for the rare occurrence of *nos-3* mutants with defects in the sperm–oocyte switch is redundancy. The *C. elegans* genome contains three predicted *nos* homologs, *nos-1*, *nos-2* and *nos-3* (Figure 1b). Each *C. elegans* NOS protein contains two putative CCHC zinc fingers at the carboxyl terminus, as well as additional conserved amino acids. The spacing of CCHC residues in NOS-3, but not in NOS-1 or NOS-2, is identical to that in *Drosophila* Nanos (Figure 1b). To test whether the three *nos* genes might encode redundant functions, we used RNAi [21] to reduce *nos-1* and *nos-2* expression, and the *nos-3*(Δ) mutant to remove *nos-3*. To obtain all possible 'mutant' combinations, *nos-1* and *nos-2* RNAs were injected either singly or in combination into either wild-type or *nos-3*(Δ) animals. The results are summarized in Table 1, and key defects are shown in Figure 4.

Table 1

Effects of removing *nos-1*, *nos-2* and *nos-3* activity.

Genotype*	Sterility†	No sperm–oocyte switch‡	Germ-line death§	Other sterile¶
Wild type	0.5	–	–	0.5
nos-3 (*n* = 2000)	0.3	0.2	–	0.1
nos-1 (*n* = 105)	13	–	–	13
nos-1 nos-3 (*n* = 124)	13	12	–	1
nos-2 (*n* = 107)	34	1	–	33
nos-2 nos-3 (*n* = 86)	34	24	–	10
nos-1 nos-2 (*n* = 463)	41	1	17	23
nos-1 nos-2 nos-3 (*n* = 231)	79	11	51	17

All animals were grown at 20°C; *nos-1* and *nos-2* mutants were obtained by RNAi; *nos-3* were *nos-3(q650)* homozygotes. The numbers shown are percentages and were from two independent experiments; although specific percentages of animals with a given defect could be variable, relative percentages were reproducible. For example, the defect in the sperm–oocyte switch was consistently 10–20-fold higher in *nos-2(RNAi) nos-3(Δ)* than in *nos-2(RNAi)* mutants. Similarly, the relative numbers of animals in each category of defects was consistent. For example, among the *nos-1 nos-2* mutants, there were always many more animals without a germ line than animals defective in the sperm–oocyte switch. Genotype* refers to *nos-3*(Δ), *nos-1(RNAi)* and *nos-2(RNAi)*. †The sum of columns 3–5. ‡Animals had a reflexed germ line with an excess of sperm that extended around the bend and no oocytes. This switch defect could not be scored in animals without a germ line. §Animals had no detectable germ-line cells when examined by Nomarski microscopy. ¶Animals with a variety of other defects leading to sterility. Most commonly, germ lines were smaller than normal with some sperm and some undifferentiated cells. This defect constituted 11% (*nos-1*), 26% (*nos-2*) or 19% (*nos-1 nos-2*) of all animals examined. In each case, the additional removal of *nos-3* reduced the percentage of animals with this phenotype markedly to 0% (*nos-1 nos-3*), 2% (*nos-2 nos-3*) and 5% (*nos-1 nos-2 nos-3*). Thus, *nos-3* appears to antagonize the effect of *nos-1* and *nos-2*. The less-common defects included feminized and tumorous germ lines as well as defects in development of the somatic gonad.

Reduction of either *nos-1* or *nos-2* strongly enhanced the defect in the sperm–oocyte switch in the *nos-3*(Δ) mutant (Table 1, column 2). The sperm–oocyte switch failure in *nos-1 nos-3* and *nos-2 nos-3* double mutants was similar to that observed in FBF-deficient [5] or *fem-3(gf)* [6] mutants: excess sperm accumulated over a larger portion of the gonad than normal and no oocytes were produced (Table 1, Figure 4a). In contrast, the *nos-1*, *nos-2* and *nos-3* single mutants were essentially wild-type for the sperm–oocyte switch (Table 1, column 2). The simplest interpretation is that these three *nos* paralogs are largely redundant in their control of the sperm–oocyte switch.

The three *nos* genes are critical for germ-line survival

In addition to a defect in the sperm–oocyte switch, *nos*-deficient animals had an additional and dramatic defect. In *nos-1 nos-2* double mutants and, at a higher frequency, in *nos-1 nos-2 nos-3* triple mutants, adults were found with no detectable germ line (Table 1, column 3; Figure 4b); *nos-1 nos-2* males were similarly lacking a germ line (data not shown). To elucidate the basis of this phenotype, we examined the germ lines of *nos-1 nos-2* and *nos-1 nos-2 nos-3* mutants during development. Most newly hatched larvae contained two germ-line precursor cells, as normal, but some had three or four germ-line precursor cells (25%, *n* = 63). The simplest interpretation is that these extra germ-line precursor cells arose by abnormally early cell division. Therefore, the *nos* genes are not required for germ-line specification during embryogenesis, but may prevent germ-line mitoses before hatching. Subsequently, in the larval L1 stage, germ-line precursor cells divided normally, but by L2 or L3, germ-line nuclei had acquired an unusual 'crinkly' or granular appearance (Figure 4c). By L4, these affected germ lines were much smaller than normal and, by adulthood, germ cells were no longer detectable (Figure 4b). We conclude that the three *nos* genes function together in promoting germ-line survival. Furthermore, because animals lacking a germ line were found after removal of *nos-1* and *nos-2*, but not with other double mutants, we speculate that *nos-1* and *nos-2* might be more critical for this control.

To determine whether the *nos* genes promote germ-line survival by preventing the programmed cell death pathway, we reduced *nos-1* and *nos-2* activities in a *ced-3* mutant background. For this experiment, *ced-3(n717)*, a strong loss-of-function allele [22], was used. The *ced-3* gene encodes a homolog of the interleukin-1β converting enzyme (ICE) protease that is required for programmed cell death [23]. We found that *ced-3(n717)*; *nos-1(RNAi) nos-2(RNAi)* mutant adults lacked germ lines (data not shown). Therefore, the *ced-3*-dependent pathway of programmed cell death is not essential for the defect in germ-line survival of *nos*-deficient animals. We conclude that a novel, *nos*-dependent pathway can control the decision between cell death and survival in germ-line tissue.

Overlapping but non-identical functions of the *nos* genes

The percentage of sterile animals among *nos-1(RNAi)* and *nos-2(RNAi)* single mutants was remarkably similar to that observed among *nos-1(RNAi) nos-3*(Δ) and *nos-2(RNAi) nos-3*(Δ) double mutants. Nevertheless, the spectrum of sterile phenotypes was different (Table 1). For example, the most prominent sterile phenotype of *nos-2* single mutants was a small germ line with some sperm and undifferentiated cells, whereas that of *nos-2 nos-3* double mutants was a larger germ line with an excess of sperm and no oocytes (see Table 1 legend). A simple interpretation is that the functions of *nos-1* and *nos-2* overlap with

Figure 4

Regulation of germ-line development by *nos*. (a) Sperm–oocyte switch. The wild-type adult germ line (left) gives rise to sperm (shown in blue) and oocytes. Some *nos*-deficient adults (right) fail to switch from spermatogenesis to oogenesis. When this happens, excess sperm are made that extend around the bend of the U-shaped germ-line tube. The *nos*-deficient animal shown is *nos-3*(Δ) *nos-1(RNAi)*. (b) Germ-cell survival. Nomarski micrographs are shown together with schematic diagrams illustrating the features relevant to this work. Upper panel, wild-type adult gonad. The adult gonadal arm is U-shaped, with a distal arm composed of mitotic and meiotic pachytene germ cells and a proximal arm with sperm and oocytes. The vulva marks the most proximal point in the gonad; somatic gonadal structures (uterus and spermatheca) are indicated. Lower panel, *nos-3*(Δ) *nos-1(RNAi) nos-2(RNAi)* gonad. No germ cells were detectable. The entire gonad was smaller than normal and the oviduct contained vacuoles that are likely to represent its lumen. (c) Germ-line nuclei at the larval L3 stage. Upper panel, wild-type germ-line nuclei are round and smooth. Lower panel, germ-line nuclei from *nos-1(RNAi) nos-2(RNAi)* animals were granular and 'crinkly'.

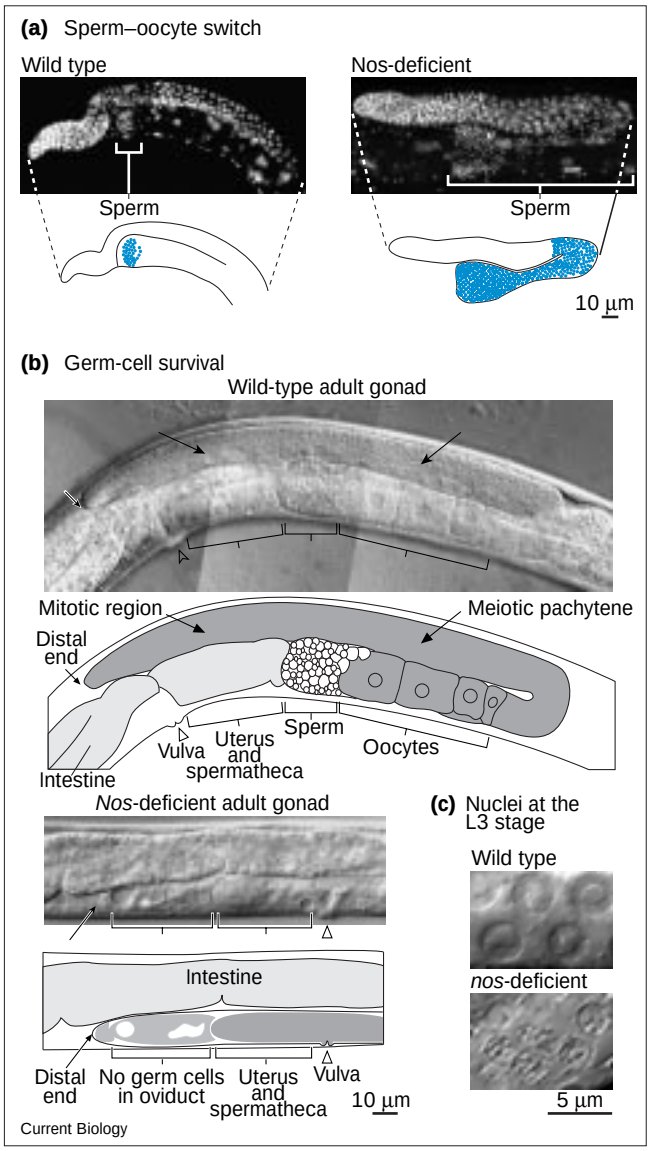

that of *nos-3* in controlling the sperm–oocyte switch, but that the individual *nos* genes also have distinct functions in the germ line. Because the effects of *nos-1* and *nos-2* that we report here were obtained using RNAi, and this method can vary from gene to gene with respect to how completely it reduces function, the quantitative impact of each *nos* gene on germ-line functions will require the isolation of null mutants in *nos-1* and *nos-2*.

Other *nos* defects

In addition to defects in the sperm–oocyte switch and germ-line survival, *nos*-deficient animals displayed germ-line defects that were not clear cell-fate transformations and also displayed ambiguous somatic gonadal malformations (Table 1, column 4 and legend). Surprisingly, however, no defects were observed in either the embryonic specification of the germ line or embryonic viability, despite the localization of NOS-3 protein to germ-line precursor cells in the embryo.

Discussion

The work reported here demonstrates that FBF and NOS-3 proteins interact physically, and that both participate in a single cell-fate decision, the sperm–oocyte switch in the hermaphrodite germ line. We suggest that FBF and NOS-3 function together in a macromolecular complex to regulate the switch in cell fate from spermatogenesis to oogenesis in *C. elegans*. FBF binds specifically to a regulatory site in the 3′UTR of *fem-3* mRNA [5], whereas NOS-3 binds RNA non-specifically (this work; also previously shown for *Drosophila* Nanos *in vitro* [18]). The FBF–NOS-3 interaction does not require RNA. These findings taken together lead to a simple model. We suggest that recruitment of NOS-3 by FBF stabilizes a regulatory complex on the *fem-3* 3′UTR (Figure 5a, left). This model cannot, however, explain the involvement of NOS-1 and NOS-2 in control of the sperm–oocyte switch, because neither NOS-1 nor NOS-2 detectably bound FBF. We therefore speculate that NOS-1 and NOS-2 form complexes with FBF indirectly, requiring either another protein or the *fem-3* 3′UTR to form a stable complex (Figure 5a, right). The relative contributions of protein–protein and protein–RNA interactions may differ between NOS-3 and the other two NOS proteins, such that NOS-1–FBF and NOS-2–FBF interactions, in the absence of RNA or the bridging protein, escape detection. Of course, more complex models are possible and include a possible association of NOS-1 and NOS-2 with other Puf proteins.

In *Drosophila*, translational repression of *hunchback* expression by the Puf protein, Pumilio, requires *nos* function [14,18]. As with NOS-1 and NOS-2, no physical interaction between the Pumilio and *Drosophila* Nanos proteins has been reported. The FBF–NOS-3 interaction leads us to suggest that proteins of the Puf and NOS families may

Figure 5

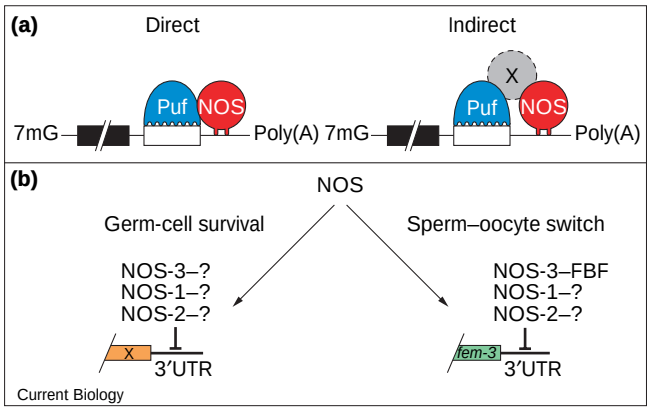

Models of NOS function in *C. elegans*. (a) A Puf–NOS–RNA regulatory complex. We propose that NOS and Puf proteins interact in a repressive complex that binds to a regulatory element (open box) in the 3′UTR. In this model, Puf proteins make sequence-specific contacts with RNA by their eight Puf repeats [5,11,13]; NOS contacts RNA non-specifically through its CCHC region ([18], this work), thereby stabilizing the complex. Left, FBF and NOS-3 interact directly. This Puf–NOS binding may further stabilize the complex. Right, PUF and NOS proteins interact indirectly through a bridging molecule, which could be either RNA or protein. In this model, we suggest the existence of a protein X. This may be the case with *Drosophila* Nanos and Pumilio, as no direct interaction has been reported to date. Similarly, we suggest that NOS-1 and NOS-2 may interact with Puf proteins in this fashion. (b) Multiple functions of *nos* genes in *C. elegans*. The *nos* genes in *C. elegans* are required for germ-line survival and for the sperm–oocyte switch. Regulation of the switch hinges on control of *fem-3* mRNA; the mRNA targets (X) that mediate survival of the germ line have not been identified. The question marks indicate as yet unknown partners of NOS proteins. Germ-line survival is proposed to be the ancestral function of the *nos* genes (see text).

generally mediate their effects by participating in protein–protein complexes bound to RNA. This view predicts that *Drosophila* Nanos functions in a complex with RNA-bound Pumilio, as proposed [13,18].

Regulation by NOS proteins in *C. elegans* is likely to be combinatorial, involving a network of protein–protein interactions and multiple mRNA targets (Figure 5b). This prediction follows from our finding that distinct developmental processes are regulated by NOS-related proteins in *C. elegans*. Here, we have focused on the sperm–oocyte switch and germ-line survival but, in addition, we have observed a defect in the mitotic arrest of germ-line precursor cells as well as post-embryonic defects in development of the somatic gonad. Furthermore, a problem with incorporation of germ-line precursor cells into the somatic gonad in animals has been observed in animals deficient for *nos-1* and *nos-2* [24]. Although FBF is required for the sperm–oocyte switch, it plays no apparent role in other *nos*-mediated effects, implying that one of the seven other *puf* orthologs in the *C. elegans* genome may provide these other functions or be redundant with FBF. Similarly, the *Drosophila pumilio* and *nos* genes have separate, but overlapping roles in germ-line development [10]. The various roles of *C. elegans nos* are likely to be mediated by regulating discrete target mRNAs. Although most of those targets have not yet been identified, they are likely to be distinct from *fem-3* mRNA, because other *nos* defects, such as germ-line death, are not observed in *fem-3* mutants [6,25]. The combinatorial nature of regulation by NOS prompts an analogy to well-documented principles of transcriptional regulation, in which distinct protein–protein interactions between transcriptional regulators discriminate among various target DNAs and yield specific biological outcomes.

Although *Drosophila nos* is best known for its role in patterning the early embryo (reviewed in [1,4,26,27]), it is also required for various aspects of germ-line development [10,15,28]. As *C. elegans* and *Drosophila nos* both control germ-line survival, we propose that the ancestral function of the *nos* genes may have been protection against germ-line death. It seems likely that the specialized roles of *nos*, such as the sperm–oocyte switch in nematodes and axis formation in *Drosophila*, were later evolutionary additions, in which a primordial regulator of germ-cell function was co-opted for other purposes, as proposed earlier by Forbes and Lehmann [10]. NOS homologs have been identified in a range of species, including vertebrates, and some are expressed in the germ line [29,30]. We speculate that these NOS proteins may be required generally for germ-line survival, as well as for idiosyncratic functions peculiar to individual species.

Conclusions

The three *C. elegans nos* genes function redundantly to control the sperm–oocyte switch and germ-line survival. FBF and NOS-3 bind to each other and both regulate the hermaphrodite sperm–oocyte switch. We suggest that these two RNA-binding proteins are physically associated in a regulatory complex that governs expression of *fem-3* mRNA. All three *C. elegans nos* genes are also critical for germ-line survival. We propose that the primordial function of *nos* genes in evolution is protection against germ-line cell death, and that their role in the sperm–oocyte switch was an idiosyncratic, evolutionary accretion.

Note added in proof

Sonada and Wharton (in press; *Genes and Development*) have demonstated that *Drosophila* Nanos and Pimilio form a tertiary complex with target RNA.

Materials and methods

Nomenclature and sequence analysis

The *nos-3* gene corresponds to Y53C12B.3 in the *C. elegans* database; *nos-1* and *nos-2* correspond to RO3D7.7 and ZK1127.1, respectively. CPB-1 is C04H1.1. Sequence comparisons and analyses were performed using the Wisconsin GCG package version 8.1 for VMS.

Generation of LambdaACT-RB-2 cDNA activation library

Poly(A)$^+$ RNA was prepared as described [31] from mixed-stage *C. elegans* hermaphrodites cultured on NGM agar plates. Random-hexamer-primed cDNA was then synthesized (Amersham Life Sciences) and purified on LMP agarose gels, eliminating small cDNAs that were < 400 bp. The cDNA was cloned into the vector Lambda ACT (a generous gift from Stephen Elledge, Baylor College of Medicine), a phage vector that allows for conversion from phage to plasmid clones using the Cre–*lox* site-specific recombination system and that allows for the propagation of the plasmid in yeast under Leu selection, with the cDNAs expressed as fusions with the yeast Gal4 activation domain. We prepared Lambda ACT to receive the cDNA by cutting the vector with the restriction enzyme *Xho*I and then filling the first base of the four-base overhang using Taq polymerase and dTTP [32]. We attached adapter sequences to the cDNA that were appropriate for the insertion into the 'T-filled' vector. The cDNA was ligated to the vector and packaged with Gigapack Gold (Stratagene). The primary library represented approximately ten million clones. All of the primary clones were amplified on the *Escherichia coli* strain LE392. A portion of the phage library was converted to plasmid by passage through the *E. coli* strain RB4E, a derivative of the strain BNN132 [32], which expresses the Cre recombinase.

Two-hybrid analyses

The yeast two hybrid-screen was carried out using yeast strain L40*ura*– as previously described [33]. Briefly, L40*ura*– yeast containing the pLexA–FBF-1 plasmid were transformed with a random-primed *C. elegans* cDNA library, LambdaACT-RB-2. The library transformation was plated on SD –trp –leu –his plates containing 5 mM 3-aminotriazole. Colonies were picked after 6 days and cDNA-containing plasmids were recovered. Recovered cDNA plasmids were reintroduced into L40 containing either pLexA–FBF-1 or pLexA–MS2 coat protein. Those cDNAs that activated expression with FBF-1, but not MS2 coat protein, were analyzed further. In directed two-hybrid tests, the vectors used were pBTM116 and pACT2 for the LexA and Gal4 activation domain plasmids, respectively. Reporter (*lacZ*) expression was assayed as previously described, using a chemiluminescent substrate [34]; β-galactosidase activities are expressed as relative light units per μg of yeast protein in the extract. Determinations were performed in triplicate.

Analysis of mRNA and sequence

The sequence of the longest cDNA, containing amino acids 42–871 of the protein, was determined by standard methods. The 5′ and 3′ termini of *nos-3* mRNA were determined using RACE protocols, essentially as described (Clontech). The *nos-1* and *nos-2* cDNAs were isolated using RT–PCR.

Purification of recombinant proteins

Recombinant proteins were purified as recommended by K. Geles and S. Adam (personal communication). Briefly, pGEX3X expression plasmids (Pharmacia) were constructed for FBF, NOS-1, NOS-2, or NOS-3 and introduced into *E. coli* strain JM109. Bacteria were grown in TB plus 2% glucose to late log phase at 37°C, induced with 1 mM IPTG for 4 h at 25°C, and harvested. All subsequent steps were at 4°C. Cells were lysed by incubation with lysozyme (0.5 mg/ml) in lysis buffer (500 mM NaCl, 5 mM DTT, 0.5 × Complete protease inhibitor cocktail (Boehringer-Mannheim), 20 mM HEPES pH 7.4). Lysates were cleared and filtered through a 0.45 μM filter. Recombinant protein was bound to glutathione sepharose (Pharmacia) and washed repeatedly with lysis buffer. Protein-bound beads were washed three times in binding buffer (see below) and used directly in pulldown assays.

GST/fusion protein affinity chromatography

In vitro protein-binding assays were performed essentially as described [35], except the binding buffer contained 0.5% non-fat dry milk, 100 mM NaCl, 5 mM DTT, 20 mM HEPES, pH 7.4. Radiolabeled (^{35}S) proteins were produced using the TNT reticulocyte lysate as directed (Promega). Labeled protein was then added to equivalent amounts of glutathione beads to which a GST fusion protein had been coupled. The amounts of coupled protein were similar for each protein analyzed, as judged by eluting a preparation of beads with SDS and staining the eluted GST protein after SDS–PAGE. Radiolabeled proteins were incubated with beads at 4°C with rocking. Beads were pelleted, washed four times in binding buffer and eluted by boiling in SDS–PAGE sample buffer. Eluted, labeled proteins were analyzed by SDS–PAGE. In the figures, the amount of material shown in lanes marked 'input' is equivalent to 10% of the amount used in the experimental lanes. For RNase A treatment (Figure 2e), ^{35}S-labeled FBF was diluted twofold in binding buffer containing RNase A to a final concentration of 5 mg/ml; a mock-treated sample lacking RNase A was also prepared. Samples were incubated for 30 min at 30°C to digest RNA. RNA was extracted from an aliquot of RNase A and mock-treated samples. RNA was analyzed by formaldehyde agarose gel electrophoresis and ethidium bromide staining as described [36]. *In vitro* protein-binding assays were performed as described above using RNase-treated samples.

Northern blotting

RNA was isolated from worms using Tri-Reagent (Molecular Research) as recommended by the manufacturer. Northern blotting using glyoxal gels was performed as described [36].

RNA-mediated interference (RNAi)

Double-stranded RNAs were transcribed using T7 polymerase (Megascript T7 kit, Ambion) from PCR-generated templates with T7 promoters at both ends. The *nos-2* RNA was 505 nucleotides long spanning exons 2–5; *nos-1* RNA was 757 nucleotides long spanning exons 2–7. These RNAs comprise most of each mRNA sequence. Single RNAs were injected at a concentration of 5.0 mg/ml, combinations of two RNAs were injected at a concentration of 2.5 mg/ml each. Progeny produced between 10 and 36 h after injection were scored.

Production of antibodies and immunofluorescence staining

Rats were injected with a keyhole-limpet-hemocyanin-coupled peptide corresponding to amino acids 679–695 of NOS-3. Antibodies were purified on a column made with the same peptide. For staining, worms were fixed according to Finney and Ruvkun [37] and embryos were fixed as described [38]. Rabbit anti-PGL-1 antibodies [20] were a gift from Susan Strome. DAPI staining was done as described in Kadyk and Kimble [39]. Anti-phospho-histone H3 antibodies were from Upstate Biotechnology; the anti-sperm antibody, SP56, was a gift from Sam Ward [40].

Isolation of deletion mutants

To induce deletion mutations, L4 hermaphrodites were treated with trimethylpsoralen and UV light as described [41]. Offspring from mutagenized animals were cultured in 1152 groups of 500. After one generation, DNA was prepared from each population, and PCR used to identify populations with animals carrying deletions in *nos-3*. Primers were: VK109 (nucleotides 26965–26986), VK110 (nucleotides 27197–27128), VK111 (nucleotides 29982–30004), and VK112 (nucleotides 30152–30173), where numbers are derived from the cosmid and span nearly the entire coding region of *nos-3*. Populations carrying a deletion were repeatedly subdivided until homozygotes carrying the deletion were obtained. Each deletion mutant was outcrossed against wild-type N2 at least six times before further characterization. Deletion endpoints were determined by sequencing PCR products that spanned the region deleted.

Acknowledgements

We thank Kuppuswamy Subramaniam and Geraldine Seydoux for communicating results before publication; Ruth Lehmann for thought-provoking discussions; and the two reviewers for excellent suggestions. We are grateful to members of the Kimble and Wickens labs for scientific and technical suggestions as well as comments on the manuscript; K. Geles and S. Adams for valuable advice on purification of bacterially expressed proteins; Susan Strome for PGL-1 antibodies; and Sam Ward for anti-sperm antibodies. We appreciate Laura Vanderploeg in the Biochemistry Media Lab for invaluable assistance in preparing figures. This work was supported by a Biotechnology Training Pre-doctoral Fellowship (B.K.), NIH

research grants (M.W., R.B., J.K.) and the American Heart Association (R.B.). J.K. is an investigator with the Howard Hughes Medical Institute.

References

1. Curtis D, Lehmann R, Zamore PD: Translational regulation and development. *Cell* 1995, 81:171-178.
2. Macdonald P, Smibert CA: Translational regulation of maternal mRNAs. *Curr Opin Genet Dev* 1996, 6:403-407.
3. Puoti A, Gallegos M, Zhang B, Wickens MP, Kimble J: Controls of cell fate and pattern by 3′ untranslated regions: the ***Caenorhabditis elegans*** sperm/oocyte decision. *Cold Spring Harb Symp Quant Biol* 1997, 62:19-24.
4. Gray NK, Wickens M: Control of translation initiation in animals. *Annu Rev Cell Dev Biol* 1998, 14:399-458.
5. Zhang B, Gallegos M, Puoti A, Durkin E, Fields S, Kimble J, *et al.*: A conserved RNA-binding protein that regulates sexual fates in the ***C. elegans*** hermaphrodite germ line. *Nature* 1997, 390:477-484.
6. Barton MK, Schedl TB, Kimble J: Gain-of-function mutations of ***fem-3***, a sex-determination gene in ***Caenorhabditis elegans***. *Genetics* 1987, 115:107-119.
7. Ahringer J, Kimble J: Control of the sperm-oocyte switch in ***Caenorhabditis elegans*** hermaphrodites by the ***fem-3*** 3′ untranslated region. *Nature* 1991, 349:346-348.
8. Lehmann R, Nüsslein-Volhard C: The maternal gene ***nanos*** has a central role in posterior pattern formation in the ***Drosophila*** embryo. *Development* 1991, 112:679-691.
9. Lin H, Spradling AC: A novel group of ***pumilio*** mutations affects the asymmetric division of germline stem cells in the ***Drosophila*** ovary. *Development* 1997, 124:2463-2476.
10. Forbes A, Lehmann R: Nanos and Pumilio have critical roles in the development and function of ***Drosophila*** germline stem cells. *Development* 1998, 125:679-690.
11. Zamore PD, Williamson JR, Lehmann R: The Pumilio protein binds RNA through a conserved domain that defines a new class of RNA-binding proteins. *RNA* 1997, 3:1421-1433.
12. Wharton RP, Struhl G: RNA regulatory elements mediate control of ***Drosophila*** body pattern by the posterior morphogen ***nanos***. *Cell* 1991, 67:955-967.
13. Murata Y, Wharton R: Binding of Pumilio to maternal ***hunchback*** mRNA is required for posterior patterning in ***Drosophila*** embryos. *Cell* 1995, 80:747-756.
14. Wharton RP, Sonoda J, Lee T, Patterson M, Murata Y: The Pumilio RNA-binding domain is also a translational regulator. *Mol Cell* 1998, 1:863-872.
15. Bhat KM: The posterior determinant gene ***nanos*** is required for the maintenance of the adult germline stem cells during ***Drosophila*** oogenesis. *Genetics* 1999, 151:1479-1492.
16. The *C. elegans* Sequencing Consortium: Genome sequence of the nematode ***C. elegans***: a platform for investigating biology. *Science* 1998, 282:2012-2018.
17. Curtis D, Apfeld J, Lehmann R: ***nanos*** is an evolutionarily conserved organizer of anterior-posterior polarity. *Development* 1995, 121:1899-1910.
18. Curtis D, Treiber DK, Tao F, Zamore PD, Williamson JR, Lehmann R: A CCHC metal-binding domain in Nanos is essential for translational regulation. *EMBO J* 1997, 16:834-843.
19. Arrizabalaga G, Lehmann R: A selective screen reveals discrete functional domains in ***Drosophila*** Nanos. *Genetics* 1999, in press.
20. Kawasaki I, Shim YH, Kirchner J, Kaminker J, Wood WB, Strome S: PGL-1, a predicted RNA-binding component of germ granules, is essential for fertility in ***C. elegans***. *Cell* 1998, 94:635-645.
21. Fire A, Xu S, Montgomery MK, Kostas SA, Driver SE, Mello CC: Potent and specific genetic interference by double-stranded RNA in ***Caenorhabditis elegans***. *Nature* 1998, 391:806-811.
22. Ellis HM, Horvitz HR: Genetic control of programmed cell death in the nematode ***C. elegans***. *Cell* 1986, 44:817-829.
23. Yuan J, Shaham S, Ledoux S, Ellis HM, Horvitz HR: The ***C. elegans*** cell death gene ***ced-3*** encodes a protein similar to mammalian interleukin-1b converting enzyme. *Cell* 1993, 75:641-652.
24. Subramaniam K, Seydoux G: ***nos-1*** and ***nos-2***, two genes related to ***Drosophila nanos***, regulate primordial germ cell development and survival in ***C. elegans***. *Development* 1999, in press.
25. Hodgkin J: Sex determination in the nematode ***C. elegans***: analysis of ***tra-3*** suppressors and characterization of ***fem*** genes. *Genetics* 1986, 114:15-52.
26. St. Johnston D, Nüsslein-Volhard C: The origin of pattern and polarity in the ***Drosophila*** embryo. *Cell* 1992, 68:201-219.
27. Macdonald P: The ***Drosophila pumilio*** gene: an unusually long transcription unit and an unusual protein. *Development* 1992, 114:221-232.
28. Kobayashi S, Yamada M, Asaoka M, Kitamura T: Essential role of the posterior morphogen ***nanos*** for germline development in ***Drosophila***. *Nature* 1996, 380:708-711.
29. Mosquera L, Forristall C, Zhou Y, King ML: A mRNA localized to the vegetal cortex of ***Xenopus*** oocytes encodes a protein with a ***nanos***-like zinc finger domain. *Development* 1993, 117:377-386.
30. Pilon M, Weisblat A: A ***nanos*** homolog in leech. *Development* 1997, 124:1771-1780.
31. Barstead RJ, Waterston RH: The basal component of the nematode dense-body is vinculin. *J Cell Biol* 1989, 264:10177-10185.
32. Elledge SJ, Mulligan JT, Ramer SW, Spottswood M, Davis RW: Lambda YES: a multifunctional cDNA expression vector for the isolation of genes by complementation of yeast and ***Escherichia coli*** mutations. *Proc Natl Acad Sci USA* 1991, 88:1731-1735.
33. Vojtek AB, Cooper JA, Hollenberg SM. Searching for interacting proteins with the two-hybrid system II. In *The Yeast Two Hybrid System*. Edited by Bartel PL, Fields S. New York: Oxford University Press; 1997:29-42.
34. Zhang B, Kraemer B, SenGupta D, Fields S, Wickens M. A yeast three-hybrid system to detect and analyze interactions between RNA and protein. In *Expression of Recombinant Genes in Eukaryotic Systems*. Edited by Glorioso JC, Schmidt MC. San Diego: Academic Press; 1999:in press.
35. Gupta MP, Amin CS, Gupta M, Hay N, Zak R: Transcription enhancer factor 1 interacts with a basic helix-loop-helix zipper protein, Max, for positive regulation of cardiac alpha-myosin heavy-chain gene expression. *Mol Cell Biol* 1997, 17:3924-3936.
36. Sambrook J, Fritsch EF, Maniatis T: *Molecular Cloning: A Laboratory Manual*, 2nd edn. New York: Cold Spring Harbor Laboratory Press; 1989.
37. Finney M, Ruvkun G: The ***unc-86*** gene product couples cell lineage and cell identity in ***C. elegans***. *Cell* 1990, 63:895-905.
38. Crittenden SL, Kimble J. Immunofluorescence methods for ***C. elegans***. In *Cell: A Laboratory Manual.* Edited by Spector D, Goldman R, Leinwand L. Cold Spring Harbor: Cold Spring Harbor Laboratory Press; 1998:108.1-108.9.
39. Kadyk LC, Kimble J: Genetic regulation of entry into meiosis in ***Caenorhabditis elegans.*** *Development* 1998, 125:1803-1813.
40. Ward S, Roberts T, Strome S, Pavalko F, Hogan E: Monoclonal antibodies that recognize a polypeptide antigenic determinant shared by multiple ***Caenorhabditis elegans*** sperm-specific proteins. *J Cell Biol* 1986, 102:1778-1786.
41. Yandel MD, Edgar LG, Wood WB: Trimethylpsoralen induces small deletion mutations in ***Caenorhabditis elegans.*** *Proc Natl Acad Sci USA* 1994, 91:1381-1385.
42. Wang C, Lehmann R: ***Nanos*** is the localized posterior determinant in ***Drosophila***. *Cell* 1991, 66:637-647.
43. SenGupta DJ, Zhang B, Kraemer B, Pochart P, Fields S, Wickens M: A three-hybrid system to detect RNA-protein interactions ***in vivo***. *Proc Natl Acad Sci USA* 1996, 93:8496-8501.
44. Gott JM, Willis MC, Koch TH, Uhlenbeck OC: A specific, UV-induced RNA-protein cross-link using 5-bromouridine-substituted RNA. *Biochemistry* 1991, 30:6290-6295.
45. Kimble JE, White JG: On the control of germ cell development in ***Caenorhabditis elegans.*** *Dev Biol* 1981, 81:208-219.
46. Austin J, Kimble J: ***glp-1*** is required in the germ line for regulation of the decision between mitosis and meiosis in ***C. elegans***. *Cell* 1987, 51:589-599.